

Expression of L-Selectin (CD62L), CD44, and CD25 on Activated Bovine T Cells

W. R. Waters,^{1*} T. E. Rahner,¹ M. V. Palmer,¹ D. Cheng,² B. J. Nonnecke,³
and D. L. Whipple¹

*Bacterial Diseases of Livestock Research Unit¹ and Periparturient Diseases of Cattle Research Unit,³
National Animal Disease Center, USDA Agricultural Research Service, Ames, Iowa 50010,
and Flow Cytometry Facility, Iowa State University, Ames, Iowa 50011²*

Received 20 June 2002/Returned for modification 7 August 2002/Accepted 15 October 2002

***Mycobacterium bovis* infection of cattle represents a natural host-pathogen interaction and, in addition to its economic and zoonotic impact, represents a model for human tuberculosis. Extravasation and trafficking of activated lymphocytes to inflammatory sites is modulated by differential expression of multiple surface adhesion molecules. However, effects of *M. bovis* infection on adhesion molecule expression have not been characterized. To determine these changes, peripheral blood mononuclear cells from *M. bovis*-infected cattle were stimulated with *M. bovis* purified protein derivative (PPD) or pokeweed mitogen (PWM) and evaluated concurrently for proliferation and activation marker expression. Stimulation with PPD or PWM increased CD25 and CD44 mean fluorescence intensity (MFI) and decreased CD62L MFI on CD4⁺ cells from infected animals. CD62L MFI on PPD- and PWM-stimulated $\gamma\delta$ T-cell receptor-positive (TCR⁺) and CD8⁺ cells was also reduced compared to that of nonstimulated $\gamma\delta$ TCR⁺ and CD8⁺ cells. Using a flow cytometry-based proliferation assay, it was determined that proliferating cells, regardless of lymphocyte subset, exhibited increased expression of CD25 and CD44 and decreased expression of CD62L compared to cells that had not proliferated. In contrast to proliferation, activation-induced apoptosis of CD4⁺ cells resulted in a significant down regulation of CD44 expression. Lymphocytes obtained from lungs of *M. bovis*-infected cattle also had reduced expression of CD44 compared to lymphocytes from lungs of noninfected cattle. These alterations in surface molecule expression upon activation likely impact trafficking to sites of inflammation and the functional capacity of these cells within tuberculous granulomas.**

Extravasation and subsequent trafficking of lymphocytes to sites of inflammation are mediated by differential expression of multiple surface adhesion molecules. L-Selectin (CD62L), for instance, mediates specific adhesion to peripheral lymph node vascular addressins (e.g., GlyCAM-1 and MAdCAM-1) targeting resting lymphocytes (CD62L^{hi}) to areas of antigen concentration within lymph nodes (16). Upon lymphocyte activation by proinflammatory cytokines, CD62L expression is down regulated and integrin (e.g., $\alpha 4\beta 1$ and $\alpha 4\beta 7$) expression and binding affinity are rapidly increased, inducing tight adhesion conducive to extravasation of lymphocytes to sites of inflammation. CD44 expression, as with integrin expression, is up regulated on lymphocytes upon activation, thereby promoting their movement through the extracellular matrix via interactions with hyaluronic acid and fibronectin (16). Indeed, anti-CD44 monoclonal antibody treatment, while not affecting leukocyte extravasation, abolishes T-cell migration to inflammatory sites (10). Actions of these adhesion molecules are modeled in vitro by stimulation of lymphocytes with antigens, anti-CD3, or mitogens resulting in down regulation of CD62L and up regulation of CD44 and $\alpha_L\beta 2$ (i.e., LFA-1) integrin expression on activated T cells (13, 16, 26, 30). Descriptions of the phenotypes of resting and activated T cells, while clear for

the mouse and human, are yet to be defined for lymphocytes of cattle.

T-cell-mediated responses are considered the hallmark of immunity to *Mycobacterium* spp., including *Mycobacterium bovis* (41, 42). A generally accepted mechanism of killing of intracellular mycobacteria is through activation of macrophages (i.e., the infected host cell) by gamma interferon (IFN- γ) produced by antigen-specific CD4⁺ T cells (21). Primary *Mycobacterium tuberculosis* infection of mice generates highly reactive CD4⁺, IFN- γ -producing cells that provide long-lived immunologic memory (2, 3). These activated CD4⁺ cells, however, are not sufficient for clearance of the primary infection of mice with this model, as antibiotic therapy is necessary for infection resolution. Upon reexposure to the pathogen following antibiotic treatment, in vivo recall CD4, IFN- γ responses are greatly accelerated and infection is controlled, suggesting that the immediate production of IFN- γ by CD4 cells is key for immune-mediated protection in the secondary response (11). Generation of this response, while essential, is ineffectual without appropriate modifications to adhesion molecule expression and signaling that affect localization and activation of CD4⁺ cells at the site of inflammation (2, 24, 27, 33). Indeed, murine CD4⁺ cells initially infiltrating *M. tuberculosis* infection sites exhibit decreased CD62L and increased CD25, CD44, and CD69 expression compared to CD4⁺ cells from noninfected animals (3, 48). Long-term immunity, however, is likely mediated by memory CD4⁺ cells that have reverted to a naïve (i.e., CD45RB^{hi} CD44^{lo} CD62L^{hi}) phenotype until restimulated with specific antigen (3).

* Corresponding author. Mailing address: United States Department of Agriculture, Agricultural Research Service, National Animal Disease Center, P.O. Box 70, Ames, IA 50010-0070. Phone: (515) 663-7756. Fax: (515) 663-7458. E-mail: rwaters@nadc.ars.usda.gov.

Studies with mice, humans, and cattle have demonstrated that CD8⁺ and $\gamma\delta$ T cells, in addition to CD4⁺ cells, are involved in the antituberculosis immune response (22, 31, 32, 38, 45, 51). Effective cytolytic activity of CD8⁺ cells, unlike trafficking and IFN- γ production by mycobacterium-specific CD8⁺ cells, requires an intact CD4⁺ cell population (49). CD8⁺ and $\gamma\delta$ T cells respond to various mycobacterial antigens and also accumulate at sites of infection, suggesting sequential expression of appropriate adhesion molecules that favor trafficking to sites of inflammation induced by the mycobacterium (5, 8, 12, 20, 29, 46, 48, 50, 54). Indeed, activated (i.e., CD44^{hi} CD62L^{lo}) CD8⁺ T cells are detected within the lungs of both tuberculous CD4^{-/-} and wild-type mice (20, 49); tuberculosis-resistant strains of mice accumulate greater numbers of CD44^{hi} CD8⁺ T cells at the site of infection (i.e., lungs) than tuberculosis-susceptible mice do (34, 35). Studies with $\gamma\delta$ T-cell receptor (TCR) gene-disrupted mice indicate that $\gamma\delta$ T cells promote the influx of lymphocytes and monocytes to infection sites and limit trafficking of tissue-damaging polymorphonuclear cells to these areas (19, 25, 37). Information concerning activation molecule expression on $\gamma\delta$ T cells responding to mycobacterial antigens compared to that of CD4⁺ and CD8⁺ cells is limited.

Tuberculosis in humans results from infection with any one of the tubercle bacilli included within the *M. tuberculosis* complex (i.e., *M. tuberculosis*, *M. bovis*, *Mycobacterium africanum*, and *Mycobacterium microti*). *M. bovis*, unlike *M. tuberculosis*, has a wide host range and is the species most often isolated from tuberculous cattle. The wide host range of *M. bovis* has made its eradication difficult, due to the presence of wildlife reservoir hosts. For instance, a recent outbreak of *M. bovis* infection in white-tailed deer in Michigan has seriously threatened *M. bovis* eradication efforts within the United States, renewing research interests in this zoonotic and economically important pathogen of domestic livestock (47). Other developed countries with wildlife reservoirs of *M. bovis* have been unable to eradicate tuberculosis from their domestic herds (6, 15) and are exploring control measures alternative to traditional test and slaughter campaigns. In addition to serious animal health and zoonotic issues, *M. bovis* infection of cattle also represents a uniquely applicable animal model for *M. tuberculosis* infection of humans.

While much is known concerning murine and human T-cell subset trafficking and activation molecule expression elicited by mycobacterial antigens, little is known about the responses of bovine lymphocytes. In cattle, distinct T-cell subsets consistently up-regulate CD25 in the recall response to mycobacterial antigen stimulation (40, 52). Additionally, $\gamma\delta$ T cells, neutrophils, CD4⁺ cells, CD8⁺ cells, and macrophages sequentially traffic to purified protein derivative (PPD) injection sites of either *M. bovis*-sensitized or *M. bovis*-infected cattle, with increased CD25 expression detected on infiltrating lymphocytes (18). In the present study, we extend these observations by determining the effects of mycobacterium-induced proliferation and apoptosis on CD25, CD44, and CD62L expression on peripheral blood T-cell subsets from *M. bovis*-infected cattle.

MATERIALS AND METHODS

Animals, bacterial culture, and challenge procedures. Twenty-five cross-bred cattle of approximately 9 months of age and obtained from herds with no history

of tuberculosis were housed at the National Animal Disease Center, USDA Agricultural Research Service, Ames, Iowa, according to the American Association of Laboratory Animal Care and institutional guidelines for animal care. At the initiation of the study, all animals were tested and confirmed negative for *M. bovis* and *Mycobacterium avium* exposure by using a commercially available assay (Bovigam; CSL Limited, Parkville, Victoria, Australia) for detection of IFN- γ production in response to mycobacterial antigen stimulation. Infected cattle ($n = 13$) were housed in temperature- and humidity-controlled rooms (1 to 2 animals/room) within a biosafety level 3 confinement facility with negative airflow exiting the building through HEPA filters. Directional airflow ensured that air from animal pens was pulled towards a central corridor and passed through HEPA filters before exiting the building. Airflow velocity was 10.4 air changes/h. Non-infected control cattle ($n = 6$) were housed similarly to infected cattle, yet in a separate building. Six additional animals housed in field barns were used as controls for studies evaluating *in vivo* expression of activation markers.

The strain of *M. bovis* used for the challenge inoculum was strain 95-1315 (USDA Animal Plant and Health Inspection Service designation) isolated originally from a white-tailed deer in Michigan in 1994 (47). Challenge inocula consisted of either $\sim 10^3$ ($n = 5$) or $\sim 10^5$ ($n = 8$) CFU of mid-log-phase *M. bovis* grown in Middlebrook 7H9 medium supplemented with 10% oleic acid-albumin-dextrose complex (Difco, Detroit, Mich.) plus 0.05% Tween 80 (Sigma Chemical Co., St. Louis, Mo.) as described previously (7). Tubercle bacilli were harvested from the culture media by centrifugation at $750 \times g$, washed twice with phosphate-buffered saline solution (PBS; 0.01 M, pH 7.2), and diluted to the appropriate cell density for use as a challenge inoculum in 2 ml of PBS. Enumeration of bacilli was by serial dilution plate counting on Middlebrook 7H11 selective medium (Becton Dickinson, Cockeysville, Md.). For aerosol inoculation, cattle were restrained and the challenge inoculum was delivered by nebulization into a mask covering the nostrils and mouth. The nebulization apparatus consisted of a compressed air tank, jet nebulizer, holding reservoir, and mask (Trudell Medical International, London, Ontario, Canada). Compressed air (25 lb/in²) was used to jet nebulize the challenge inoculum (2 ml of *M. bovis* in PBS) directly into the holding reservoir. Upon inspiration, the nebulized inoculum was inhaled through a one-way valve into the mask and directly into the nostrils. A rubber gasket sealed the mask securely to the muzzle, preventing leakage of inoculum around the mask. Expired air exited through one-way valves on the sides of the mask. The nebulization process continued until all of the inoculum, a 1-ml PBS wash of the inoculum tube, and an additional 2 ml of PBS were delivered (~ 12 min). Strict biosafety level 3 protocols were followed to protect personnel from exposure to *M. bovis*. At the conclusion of the experiment, cattle were euthanized by intravenous administration of sodium pentobarbital (Sleepaway; Fort Dodge Laboratories).

Mononuclear cell culture and PKH67 staining. Peripheral blood mononuclear cells (PBMC) were isolated from buffy coat fractions of blood collected in 2 \times acid-citrate-dextrose (9). Staining of PBMC with PKH67 was performed according to the manufacturer's instructions (Sigma) and as described elsewhere (56–58). Briefly, 2×10^7 PBMC were centrifuged (10 min, $400 \times g$), supernatants were aspirated, and cells were resuspended in 1 ml of the diluent provided in the PKH67 kit. Cells in diluent were added to 1 ml of PKH67 green fluorescent dye (2 μ M) and incubated for 5 min, followed by a 1-min incubation with 2 ml of fetal bovine sera (FBS) to adsorb the excess dye and stop further dye uptake by cells. Cells were then washed (twice) with RPMI 1640, and wells of 96-well round-bottom microtiter plates (Falcon; Becton-Dickinson, Lincoln Park, N.J.) were seeded with 2×10^5 PKH67-stained mononuclear cells in a total volume of 200 μ l per well (6 to 12 replicates for each treatment). Medium was RPMI 1640 supplemented with 25 mM HEPES buffer, 100 U of penicillin/ml, 0.1 mg of streptomycin/ml, 50 μ M 2-mercaptoethanol (Sigma), and 10% (vol/vol) heat-inactivated (56°C, 30 min) FBS. Wells contained medium plus 5 μ g of *M. bovis* PPD (CSL Limited)/ml, 1 μ g of pokeweed mitogen (PWM)/ml, or medium alone (no stimulation). Cultures were incubated at 37°C in 5% CO₂ in air.

Cell surface marker, Annexin V, and 7AAD staining for flow cytometry. Cells were harvested after 0, 3, 5, and 7 days of culture from wells and pooled for individual animals according to treatment (i.e., 6 to 12 replicates pooled per treatment). Approximately 2×10^5 pooled cells in 200 μ l of culture medium were added to individual wells of round-bottom microtiter plates, centrifuged (2 min, $400 \times g$), and resuspended in 100 μ l of primary antibody(s) (~ 1 μ g/well) in PBS containing 1% FBS and 0.1% sodium azide (fluorescence-activated cell sorter [FACS] buffer). Primary antibodies included anti-CD4 (GC50A1; immunoglobulin M [IgM]), anti-CD8 α (BAQ111A; IgM), anti- $\gamma\delta$ TCR (GB21A, specific for the δ chain; IgG2b), anti-CD25 (CACT116A, IgG1), anti-CD44 (BAT31A; IgG1), and anti-CD62L (BAQ92A; IgG1) (all obtained from VMRD, Pullman, Wash.). After a 15-min incubation at room temperature, cells were centrifuged (2 min, $400 \times g$) and resuspended in 100 μ l each of Cyanine 5 (CY 5; 2

TABLE 1. Flow cytometry staining (five-color) protocol

Analysis	Reagent or antibody added to tube no.								
	1	2	3	4	5	6	7	8	9
Proliferation	PKH67	PKH67	PKH67	PKH67	PKH67	PKH67	PKH67	PKH67	PKH67
Phenotype									
Primary antibody	CD4	CD8	$\gamma\delta$ TCR	CD4	CD8	$\gamma\delta$ TCR	CD4	CD8	$\gamma\delta$ TCR
Secondary antibody	IgM-PE	IgM-PE	IgG2b-PE	IgM-PE	IgM-PE	IgG2b-PE	IgM-PE	IgM-PE	IgG2b-PE
Activation									
Primary antibody	CD62L	CD62L	CD62L	CD44	CD44	CD44	CD25	CD25	CD25
Secondary antibody	IgG1-CY5	IgG1-CY5	IgG1-CY5	IgG1-CY5	IgG1-CY5	IgG1-CY5	IgG1-CY5	IgG1-CY5	IgG1-CY5
Apoptosis ^a									
Primray antibody	Annexin V	Annexin V	Annexin V	Annexin V	Annexin V	Annexin V	Annexin V	Annexin V	Annexin V
Secondary antibody	RED613 or ECD	RED613 or ECD	RED613 or ECD	RED613 or ECD	RED613 or ECD	RED613 or ECD	RED613 or ECD	RED613 or ECD	RED613 or ECD

^a 7AAD was also included for further discrimination of early apoptotic and dead cells.

$\mu\text{g}/\text{well}$)-conjugated goat anti-mouse IgG1 and phycoerythrin (PE; 1 $\mu\text{g}/\text{well}$)-conjugated goat anti-mouse IgM or IgG2b (Southern Biotechnology Associates, Birmingham, Ala.). Cells in secondary antibody were incubated for 15 min at room temperature in the dark, washed with FACS buffer, and resuspended in 200 μl of Annexin V binding buffer (Pharmlingen, San Diego, Calif.) containing 2 μg of biotin-labeled Annexin V (Pharmlingen). Cells were incubated for 15 min and washed, and 100 μl of streptavidin-RED613 or streptavidin-ECD (1 to 2 $\mu\text{g}/\text{well}$; Texas Red-PE tandem dyes) was added to each well. After a 15-min incubation, cells were centrifuged (400 \times g, 2 min) and resuspended in Annexin V binding buffer containing 7-amino-actinomycin D (7AAD; 1 $\mu\text{g}/\text{well}$; Molecular Probes, Eugene, Oreg.). The staining protocol for the five-color procedure is outlined in Table 1.

Three-color analysis, as previously described (58), was also performed on cultured PKH67-stained PBMC and freshly isolated, non-PKH67-stained cells obtained from lungs, mediastinal lymph nodes, and prefemoral lymph nodes at necropsy. Cells were stained as described above, although peridinin chlorophyll protein (PerCP)-conjugated rat anti-mouse IgG1 (Becton Dickinson) was used as a secondary reagent for activation molecules (i.e., CD25, CD44, and CD62L) in place of the CY 5 conjugate. Additionally, Annexin V-PE (2 μg ; Pharmlingen) and 7AAD staining was performed on cells in wells other than those receiving antibodies to surface markers. Anti-CD3 (MM1A; VMRD) and anti-IgM (PIG45A; VMRD) were included in addition to anti-CD4, anti-CD8 α , anti- $\gamma\delta$ TCR, anti-CD25, anti-CD44, and anti-CD62L. Since cells collected from tissues were not PKH67 stained, fluorescein isothiocyanate-conjugated goat anti-mouse IgG1 (Pharmlingen) was used in place of the PerCP conjugate.

Flow cytometric analysis. An EPICS ALTRA HyPerSort system flow cytometer (Beckman Coulter, Miami, Fla.) was aligned with an air-cooled argon laser beam (488 nm at 15 mW) as the first beam and an air-cooled red helium neon laser (633 nm at 10 mW) spatially separated from the argon beam by 20 μs . Fluorescence signals of PKH67, PE, RED613/ECD, and 7AAD were excited by using the 488-nm beam and CY 5 was excited by using the 633-nm beam. Forward scatter and side scatter were measured through 488-nm band-pass (BP) filters allowing only the detection of the 488-nm argon laser light scatter. A dichroic 550 long-pass filter was used to spectrally separate PKH67 fluorescence detection to photomultiplier tube 2 (PMT2) (525-nm BP). A dichroic 600 long-pass filter separated the PE signal to PMT3 (575-nm BP), and a dichroic 640 long-pass signal reflected the PE-Texas Red tandem dye signal to PMT4 (610-nm BP). The long red signals (CY 5 and 7AAD) were collected on PMT5 through a 675-nm BP filter. The fluorescent and scatter signals originating from the 488-nm beam (FS, SS, PKH67, PE, RED613, and 7AAD) were delayed for 20 μs , and the long red signals (CY 5 and 7AAD) were discriminated from one another using the gated amplifier with auxiliary signal processing for CY 5 fluorescence. Single- or dual-color samples stained with either PKH67 only or PKH67 with PE, RED613/ECD, CY 5, or 7AAD were used to optimize compensation between the PMTs. For three-color analysis, data were acquired using a Becton Dickinson FACScan flow cytometer (10,000 events; live gate; 488-nm laser). Modfit Proliferation Wizard (Verity Software House Inc., Topsham, Maine), CellQuest software (Becton Dickinson), and FlowJo (Tree Star Inc., San Carlos, Calif.) were used for cell proliferation and phenotype analyses. Proliferation profiles were determined for both gated (i.e., CD4⁺, CD8⁺, or $\gamma\delta$ TCR⁺) and ungated (total

PBMC) populations. Data are presented as the mean (\pm standard error of the mean [SEM]) number of cells that had proliferated per 10,000 PBMC, as geometric mean fluorescence intensities, or as percent positive-staining cells.

Collection of leukocytes from tissues. Cells were collected from prefemoral and mediastinal lymph nodes and lungs of infected ($n = 10$) and noninfected ($n = 9$) cattle at necropsy by scraping tissues over a stainless steel mesh into FACS buffer. Cells were further disrupted by moderate and repeated expulsion from a 10-ml syringe through a 20-gauge needle against a petri dish. Cells were diluted to $\sim 2 \times 10^6/\text{ml}$, stained, fixed with 2.0% paraformaldehyde, and analyzed as described above for three-color flow cytometric analysis of lymphocyte subsets.

Statistics. Data were analyzed by either a one-way analysis of variance followed by the Tukey-Kramer multiple-comparison test or Student's t test using a commercially available statistics program (InStat 2.00; GraphPAD Software, San Diego, Calif.).

RESULTS

CD4⁺ and $\gamma\delta$ TCR⁺ PBMC from *M. bovis*-infected cattle proliferate in response to *M. bovis* antigen stimulation. Aerosolization of *M. bovis* into cattle resulted in gross and microscopic lesions in all animals regardless of the dose; however, lesions were more extensive and severe in cattle receiving 10^5 CFU than in cattle receiving 10^3 CFU. Lesions were most prominent in the lungs and lung-associated lymph nodes (i.e., mediastinal and tracheobronchial). As previously demonstrated (57, 58), recall proliferation of PBMC from *M. bovis*-infected cattle in response to *M. bovis* PPD was primarily the result of proliferation by CD4⁺ and $\gamma\delta$ TCR⁺ cells (Table 2). Differences in proliferative responses between challenge doses (i.e., 10^3 versus 10^5 CFU) were not detected; thus, data are presented as pooled analyses. Proliferation of CD8⁺ cells in response to PPD exceeded ($P < 0.002$) that of CD8⁺ cells to media alone. Proliferation of either CD4⁺ or $\gamma\delta$ TCR⁺ cells to PPD exceeded ($P < 0.01$) that of CD8⁺ cells to PPD. Additionally, there were greater ($P < 0.002$) numbers of CD4⁺ cells in PPD-stimulated cultures than in nonstimulated cultures (i.e., 2,836 for PPD-stimulated versus 753 for nonstimulated cultures, with values expressed as the mean per 10,000 live PBMC), further evidence of expansion of this subset in response to PPD.

CD25, CD44, and CD62L expression on antigen-stimulated bovine T-cell subsets. To evaluate the effects of antigenic stimulation on CD25, CD44, and CD62L expression by bovine T-cell subsets, PBMC isolated from *M. bovis*-infected cattle (n

TABLE 2. Lymphocyte subset proliferative responses of *M. bovis*-infected cattle^a

Condition	Total	CD4 ⁺	CD8 ⁺	$\gamma\delta$ TCR ⁺
Nonstimulated	1,175 \pm 134	138 \pm 21	29 \pm 4	453 \pm 81 ^d
PPD stimulated	4,922 \pm 487 ^c	2,603 \pm 480 [*]	118 \pm 13 ^{*e}	1,621 \pm 289 [*]
Fold increase in proliferation ^b	4.2	18.9	4.2	13.6

^a Cattle ($n = 10$) were infected with *M. bovis* via aerosolization. Mononuclear cells were harvested, stained with PKH67, incubated with media alone (i.e., nonstimulated) or with 5 μ g of *M. bovis* PPD/ml (i.e., PPD stimulated) for 6 days, stained with cell surface markers for flow cytometry, and analyzed for proliferation (i.e., decreased PKH67 staining intensity) in conjunction with detection of lymphocyte surface markers. Dead cells (i.e., 7AAD^{bright}) were excluded from analysis. Data represent the mean (\pm SEM) number of cells that had proliferated per 10,000 PBMC, and results are representative of two independent experiments.

^b Fold increase in proliferation of PPD-stimulated samples in relation to nonstimulated samples.

^c *, differs ($P < 0.002$) from responses of nonstimulated samples (i.e., vertical comparisons).

^d Differs ($P < 0.05$) from responses of nonstimulated CD4⁺ or CD8⁺ samples (i.e., horizontal comparisons).

^e Differs ($p < 0.01$) from responses of PPD-stimulated CD4⁺ or $\gamma\delta$ TCR⁺ samples (i.e., horizontal comparisons).

= 3; 10^5 CFU) were stimulated with *M. bovis* PPD and harvested periodically for flow cytometric analysis. CD25 and CD44 fluorescence increased and CD62L fluorescence decreased on CD4⁺ cells from PPD-stimulated cultures (Fig. 1) compared to that of nonstimulated cultures (Fig. 1). CD25

fluorescence of $\gamma\delta$ TCR⁺ cells from PPD-stimulated cultures compared to those from nonstimulated cultures was increased (Fig. 1). T-cell subsets were also evaluated for CD25, CD44, and CD62L expression after 0, 3, 5, and 7 days of culture (i.e., longitudinal responses) with or without PPD (Fig. 2 presents

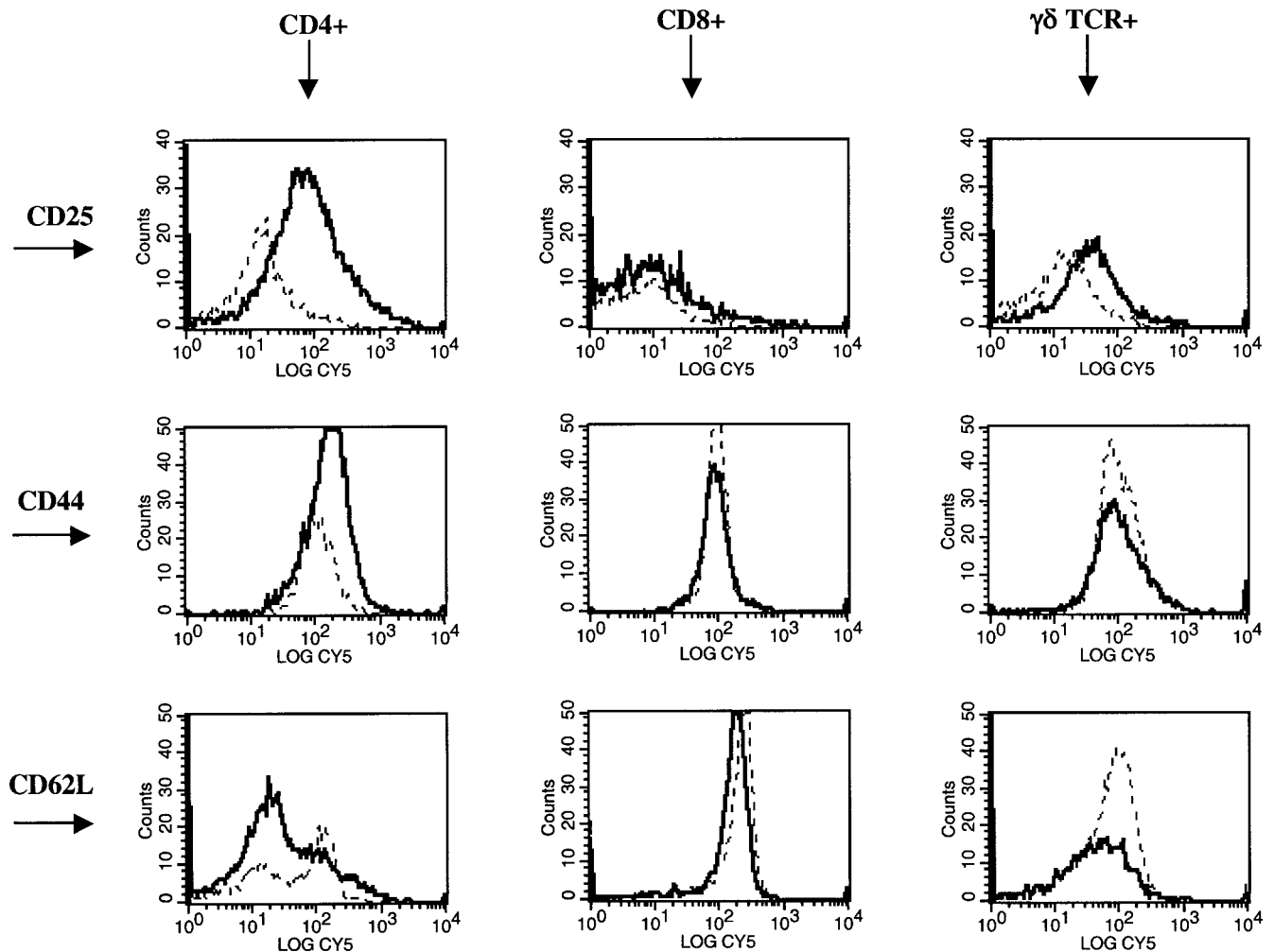


FIG. 1. Histogram overlays demonstrating CD25, CD44, and CD62L expression on bovine T-cell subsets. Mononuclear cells were isolated and cultured with no stimulation (dotted lines) or 5 μ g of *M. bovis* PPD/ml (dark solid lines) for 5 days. After 5 days of culture, cells were harvested and stained for five-color analysis as described in Materials and Methods. Gates were set on live (i.e., Annexin V⁻ 7AAD⁻) and CD4⁺, CD8⁺, or $\gamma\delta$ TCR⁺ cells. Histograms represent the log fluorescence (CY 5) of CD4⁺, CD8⁺, or $\gamma\delta$ TCR⁺ cells stained with either anti-bovine CD25, CD44, or CD62L.

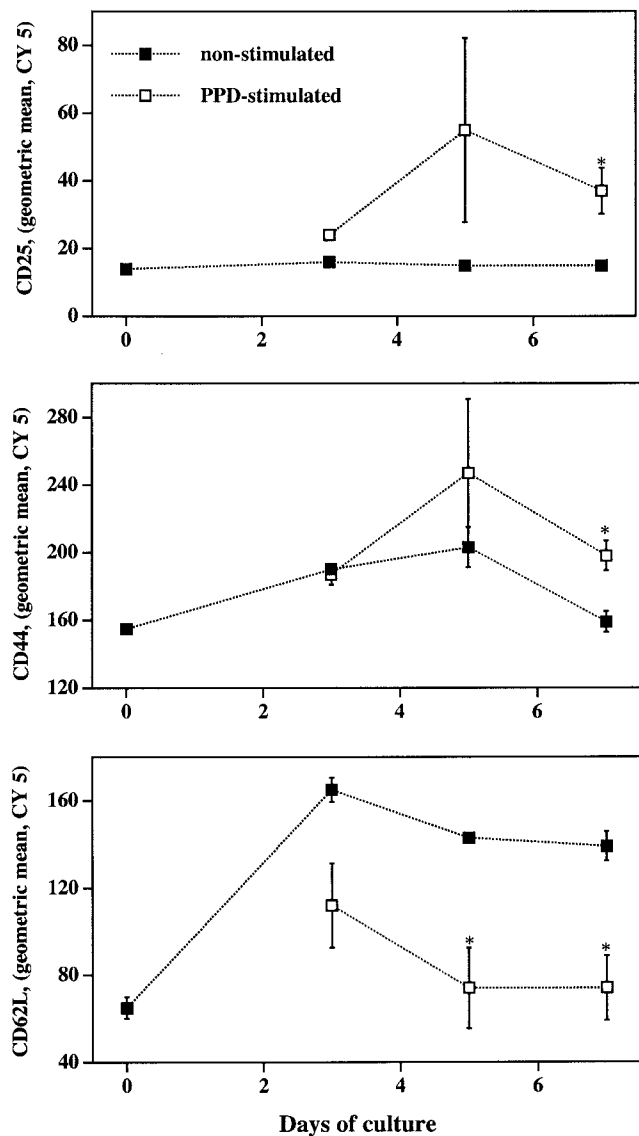


FIG. 2. In vitro kinetics of CD25, CD44, and CD62L expression on bovine CD4⁺ T cells. Mononuclear cells were isolated and cultured with no stimulation (closed boxes) or with 5 µg of *M. bovis* PPD/ml (open boxes) and harvested at days 0, 3, 5, and 7 of culture for flow cytometric analysis. Live (i.e., Annexin V⁻ 7AAD⁻) CD4⁺ (PE⁺) cells were analyzed to determine the geometric mean fluorescence (CY 5) intensity of CD25, CD44, or CD62L expression. Data are presented as means (± SEM; n = 3) of the geometric CY 5 intensity. *, differs (P < 0.05) from nonstimulated samples at the same time point.

the responses of CD4⁺ cells). From this analysis, it was determined that differences in expression of these molecules on PPD-stimulated versus nonstimulated cells were maximal between 5 and 7 days of culture. Alterations in CD25, CD44, and CD62L expression upon PPD stimulation on cells from non-infected cattle were not detected (data not shown).

To further evaluate this response with a larger population, PBMC were harvested from 10 animals infected with *M. bovis* via aerosolization, with five receiving 10³ CFU of *M. bovis* and five receiving 10⁵ CFU of *M. bovis*. Effects (P < 0.05) of challenge dose were not detected; therefore, data obtained

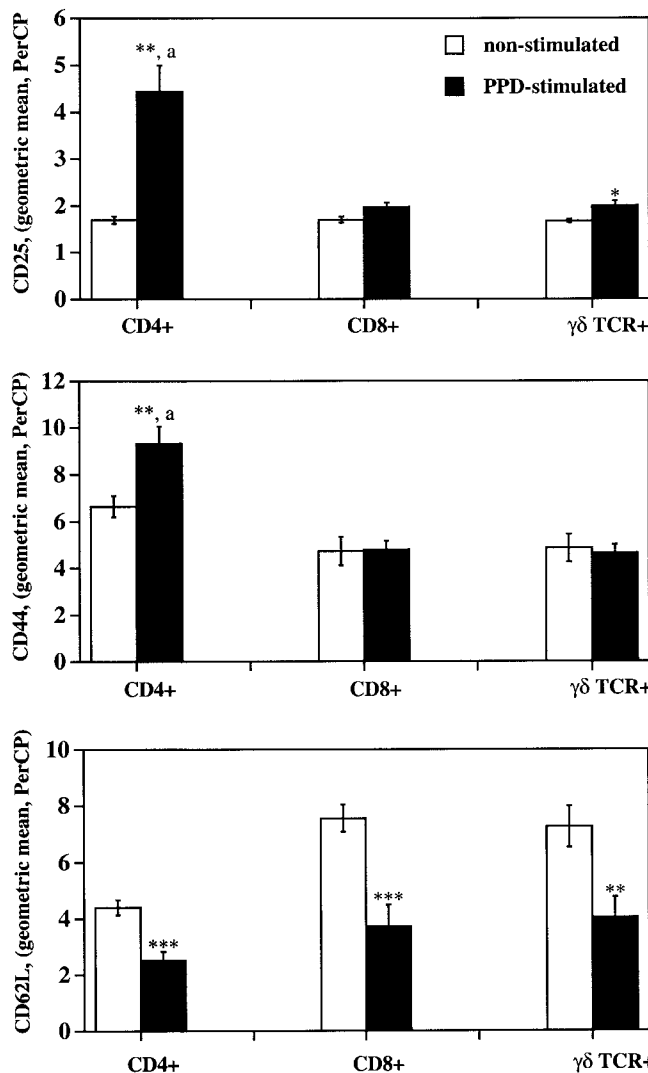


FIG. 3. Mean fluorescence intensity (PerCP) of activation markers on nonstimulated and PPD-stimulated T-cell subsets from *M. bovis*-infected cattle. Isolated mononuclear cells were incubated with media alone (i.e., nonstimulated; open bars) or 5 µg of *M. bovis* PPD/ml (i.e., PPD-stimulated; closed bars) for 6 days and analyzed for CD4, CD8, or γδ TCR expression (PE) as well as CD25, CD44, or CD62L expression (PerCP). For analysis, gates were set on live (i.e., forward and side scatter properties of Annexin V⁻ 7AAD⁻ cells) and T-cell subset marker-positive (i.e., CD4⁺, CD8⁺, or γδ TCR⁺ cells) cells, and the geometric mean fluorescence intensity (PerCP) of CD25, CD44, or CD62L expression was determined. Data are presented as means (± SEM; n = 10). P values for differences from nonstimulated samples for the respective T-cell subset (i.e., comparisons between open and closed bars for each graph) were as follows: *, P < 0.05; **, P < 0.01; ***, P < 0.001. "a" indicates differences (P < 0.01) from expression by PPD-stimulated CD8⁺ and γδ TCR⁺ cells for the respective activation marker (i.e., comparisons between closed bars for each graph).

from these 10 animals, as with the proliferation data, were pooled for further analyses (Fig. 3 and 4). A single time point (i.e., 6 days) was evaluated, as this was determined to be an optimal time point from the initial experiment with a limited number of animals. Again, the fluorescence intensity of CD25 and CD44 increased (P < 0.01) and that of CD62L decreased (P < 0.001) on CD4⁺ cells upon PPD stimulation (Fig. 3).

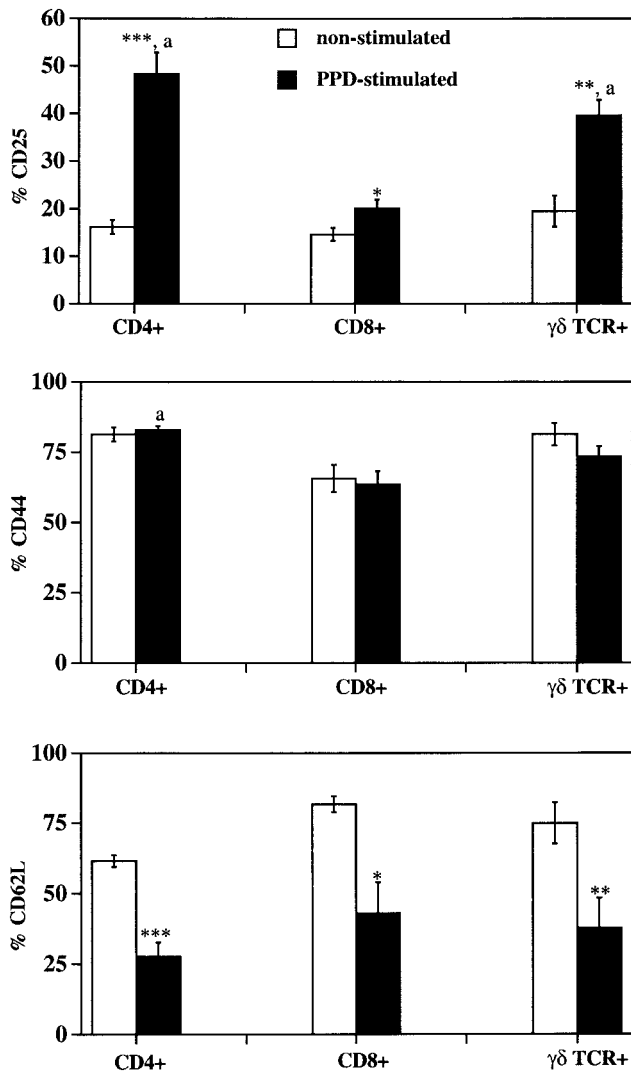


FIG. 4. Percent activation marker expression on nonstimulated and PPD-stimulated T-cell subsets from *M. bovis*-infected cattle. Isolated mononuclear cells were incubated with media alone (i.e., nonstimulated; open bars) or 5 μ g of *M. bovis* PPD/ml (i.e., PPD stimulated; closed bars) for 6 days and analyzed for CD4, CD8, or $\gamma\delta$ TCR expression (PE) as well as CD25, CD44, or CD62L expression (PerCP). The percent CD25⁺, CD44⁺, or CD62L⁺ cells was determined for live (i.e., forward and side scatter properties of Annexin V⁻ 7AAD⁻ cells) and T-cell subset marker-positive (i.e., CD4, CD8, or $\gamma\delta$ T cells) cells. Data are presented as means (\pm SEM; $n = 10$). *P* values for differences from nonstimulated samples for the respective T-cell subset (i.e., comparisons between open and closed bars for each graph) were as follows: *, $P < 0.05$; **, $P < 0.01$; ***, $P < 0.001$. "a" indicates differences ($P < 0.01$) from expression by PPD-stimulated CD8⁺ cells for the respective activation marker subset (i.e., comparisons between closed bars for each graph).

Compared to nonstimulated cultures, PPD-stimulated cultures had increased ($P < 0.001$) percentages of CD4 cells positive for CD25 and decreased ($P < 0.001$) percentages of CD4 cells positive for CD62L (Fig. 4). The percentage of cells expressing CD44, regardless of the subset, was not affected by PPD stimulation. Expression of CD25 increased and CD62L decreased (i.e., fluorescence intensity and percent positive) on $\gamma\delta$ TCR⁺ cells upon PPD stimulation (Fig. 3 and 4). The mean fluores-

cence intensities of CD25 and CD44 on PPD-stimulated CD4⁺ cells were greater ($P < 0.01$) than those of either PPD-stimulated $\gamma\delta$ TCR⁺ or PPD-stimulated CD8⁺ cells (Fig. 3). Differences in CD25, CD44, and CD62L expression described above were not detected when cells from noninfected cattle ($n = 3$) were evaluated, indicating the antigen-specific nature of this response (data not shown). Upon PWM stimulation, CD25 expression increased and CD62L expression decreased on CD4⁺, $\gamma\delta$ TCR⁺, and CD8⁺ cells. CD44 expression also increased on PWM-stimulated CD4⁺ and CD8⁺ cells compared to nonstimulated cells (data not shown).

Evaluation of CD25, CD44, and CD62L expression on proliferative (i.e., PKH67^{dim}) cells. To determine if proliferation affects CD25, CD44, and CD62L expression, PKH67-stained PBMC were cultured with or without PPD and harvested for flow cytometric analysis. PKH67 is a fluorochrome with an aliphatic tail that readily incorporates into the lipid bilayer of the cell membrane. As cells divide, PKH67 staining intensity diminishes, resulting in a decreased mean fluorescence intensity of PKH67 on proliferative compared to nonproliferative cells (4). The stability of the dye incorporation into the lipid membrane ensures that as cells divide the dye is distributed equally between daughter cells. Significant ($P < 0.05$) increases in CD25 and CD44 and decreases in CD62L fluorescence intensity were detected on proliferative (i.e., PKH67^{dim}) compared to nonproliferative (i.e., PKH67^{bright}) fractions for each T-cell subset evaluated, with one exception (Fig. 5). CD62L expression on PKH67^{bright} and PKH67^{dim} CD4⁺ cells did not differ ($P < 0.05$). CD25 and CD44 expression on proliferative (i.e., PKH67^{dim}) CD4⁺ cells did, however, exceed ($P < 0.05$) that of proliferative $\gamma\delta$ TCR⁺ or CD8⁺ cells. Evaluation of total PBMC (i.e., regardless of subset) revealed increases ($P < 0.002$) in expression of CD25 and CD44 and decreases ($P = 0.066$) in expression of CD62L on proliferative (i.e., PKH67^{dim}) versus nonproliferative (i.e., PKH67^{bright}) fractions (data not shown).

CD25, CD44, and CD62L expression on antigen-stimulated Annexin V⁺ 7AAD^{dim} (i.e., early apoptotic) cells. A natural sequela of antigen-specific proliferation, among other fates, is apoptosis (1). To accurately delimit live, early apoptotic, and dead cells for prohibitive analyses, gates were set based upon Annexin V and 7AAD staining properties (Fig. 6). Proliferation to either PPD or PWM stimulation resulted in increased percentages of early apoptotic (i.e., Annexin V⁺ 7AAD^{dim/-}; gate R2) cells (Fig. 6). CD25 and CD62L expression on Annexin V⁻ 7AAD⁻ (i.e., live) and Annexin V⁺ 7AAD^{dim/-} (i.e., early apoptotic) PPD-stimulated CD4⁺ cells did not differ (data not shown). Live (i.e., Annexin V⁻ 7AAD⁻) PWM-stimulated CD4⁺ cells had moderately increased ($P = 0.1$) CD25 fluorescence intensity and decreased ($P < 0.01$) CD62L fluorescence intensity after 5 days of stimulation compared to that of early apoptotic (i.e., Annexin V⁺ 7AAD^{dim/-}) PWM-stimulated CD4⁺ cells (data not shown). CD44 fluorescence intensity, however, was increased ($P < 0.05$) on both PPD- and PWM-stimulated CD4⁺ Annexin V⁻ 7AAD⁻ cells compared to that of CD4⁺ Annexin V⁺ 7AAD^{dim/-} cells, indicating significant down regulation of this molecule with early apoptosis (Table 3).

CD25, CD44, and CD62L expression on mononuclear cells isolated from lung and lymph nodes of *M. bovis*-infected ani-

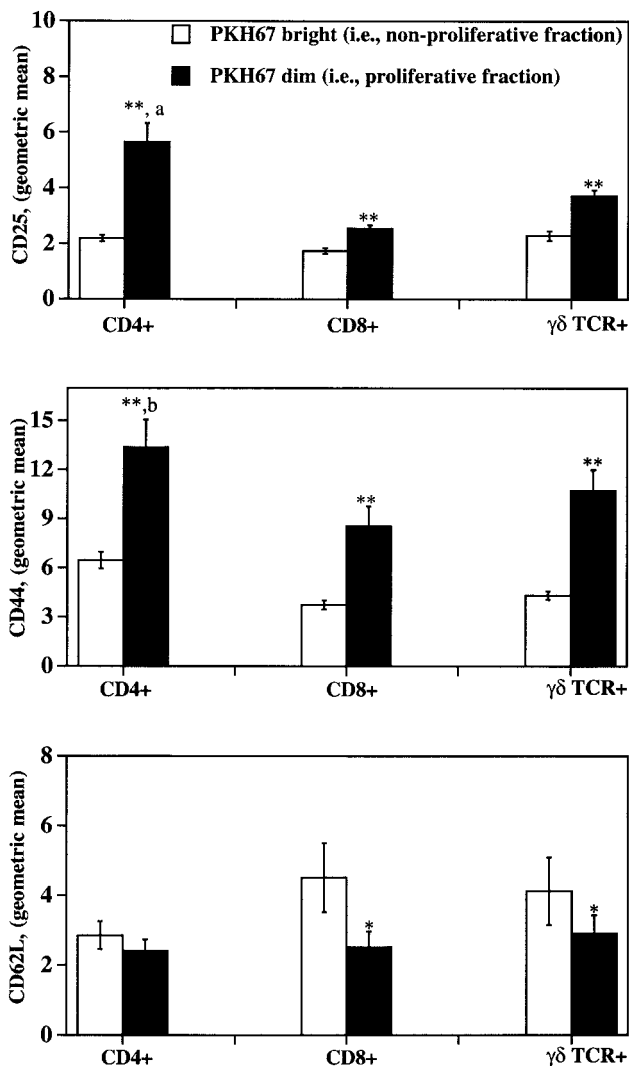


FIG. 5. Mean fluorescence intensity (PerCP) of activation markers on PPD-stimulated, PKH67^{bright} (i.e., nonproliferative fraction; open bars) or PKH67^{dim} (i.e., proliferative fraction; closed bars) T-cell subsets from *M. bovis*-infected cattle. Isolated mononuclear cells were stained with PKH67 and incubated with 5 μ g of *M. bovis* PPD/ml for 6 days and analyzed for PKH67 staining intensity (FL-1 channel); CD4, CD8, or $\gamma\delta$ TCR expression (FL-2 channel; PE); and CD25, CD44, or CD62L expression (FL-3 channel; PerCP). The geometric mean fluorescence intensity (PerCP) of CD25, CD44, or CD62L expression was determined for individual T-cell subsets (i.e., CD4⁺, CD8⁺, or $\gamma\delta$ TCR⁺ cells), with further discrimination based on PKH67 staining intensity (i.e., bright or dim). Only cells with light scatter properties typical of live cells (i.e., Annexin V⁻ 7AAD⁻) were evaluated. Data are presented as means (\pm SEM; $n = 10$). *P* values for differences from PKH67^{bright} fractions for the respective T-cell subset (i.e., comparisons between open and closed bars for each graph) were as follows: *, *P* < 0.05; **, *P* < 0.01; ***, *P* < 0.001. "a" indicates difference (*P* < 0.05) from expression by PPD-stimulated CD8⁺ and $\gamma\delta$ TCR⁺ cells; "b" indicates difference (*P* < 0.05) from expression by PPD-stimulated CD8⁺ cells for the respective activation marker (i.e., comparisons between closed bars for each graph).

mals. To evaluate in vivo expression of CD25, CD44, and CD62L on T cells within *M. bovis*-infected cattle, cells were harvested from tissues collected from infected ($n = 10$) and noninfected ($n = 9$) cattle at necropsy and evaluated by flow

cytometry. Tissues included lung and mediastinal lymph nodes (i.e., tissues colonized by *M. bovis* and with granulomatous lesions) and prefemoral lymph nodes (i.e., *M. bovis* not detected and no lesions). Expression of CD25 by mononuclear cells isolated from infected and noninfected cattle did not differ (*P* > 0.05). Mononuclear cells collected from lungs of infected cattle had decreased (*P* < 0.05) expression of CD44 and CD62L compared to that of noninfected cattle (Table 4). Mediastinal lymph node cells of infected cattle also had decreased (*P* < 0.01) expression of CD62L compared to that of noninfected cattle (Table 4). CD44 and CD62L expression on prefemoral lymph node cells of infected and noninfected cattle did not differ (*P* > 0.05; data not shown).

DISCUSSION

Bacilli of the tuberculosis complex induce severe granulomatous inflammation characterized by trafficking of numerous activated T cells to sites of bacterial infection. Trafficking, activation, proliferation, and apoptosis of mycobacterium-specific lymphocytes are quintessential in the tubercular immune response, and these responses are often employed to demonstrate the basic features of antigen-induced, cell-mediated immune responses. In the present study, PBMC isolated from cattle infected with *M. bovis* (i.e., a natural host-pathogen relationship) were used to evaluate bovine CD25, CD44, and CD62L expression upon polyclonal activation and proliferation. Antigen-stimulated CD4⁺ cells down regulated CD62L and up regulated CD25 and CD44 expression. Bovine CD8⁺ and $\gamma\delta$ TCR⁺ cells, likewise, exhibited decreased CD62L and increased CD25 expression upon activation; CD44 expression on these two subsets, however, did not change. Analysis of CD44 expression of proliferative (i.e., PKH67^{dim}) CD8⁺ or $\gamma\delta$ TCR⁺ cell fractions compared to that of nonproliferative (i.e., PKH67^{bright}) CD8⁺ or $\gamma\delta$ TCR⁺ cell fractions, conversely, indicated that up regulation of CD44 does occur upon proliferation of these two T-cell subsets. With this type of analyses, surface expression of activation molecules on minor, less-expanded subpopulations can be determined separately from that of nonresponder cells, thereby revealing subtle changes in the phenotype of proliferating subsets. These findings are consistent with prior studies examining CD25 expression on proliferating bovine T cells (43, 52, 53) yet inconsistent with another observation that CD62L expression is not altered on phorbol myristate acetate (PMA)-ionomycin-stimulated bovine T cells (28). Another group, however, has demonstrated that PMA stimulation does induce a significant down regulation of CD62L on bovine $\alpha\beta$ T cells, with a less pronounced, yet measurable, similar effect on $\gamma\delta$ T cells (55). Presently we extend these findings, demonstrating that, as with murine T cells, bovine T cells also down regulate CD62L and up regulate CD25 and CD44 upon in vitro stimulation with mycobacterial antigens (2, 3, 24, 27, 33, 48). Mechanisms underlying alterations in CD44 or CD62L expression, however, were not addressed.

The in vivo consequences of CD25 and CD44 up regulation and CD62L shedding in response to mycobacterial antigen stimulation on bovine T cells are unknown. Certainly, T cells within tissues of chronically infected cattle are continuously stimulated by mycobacterial antigens as well as by cytokines

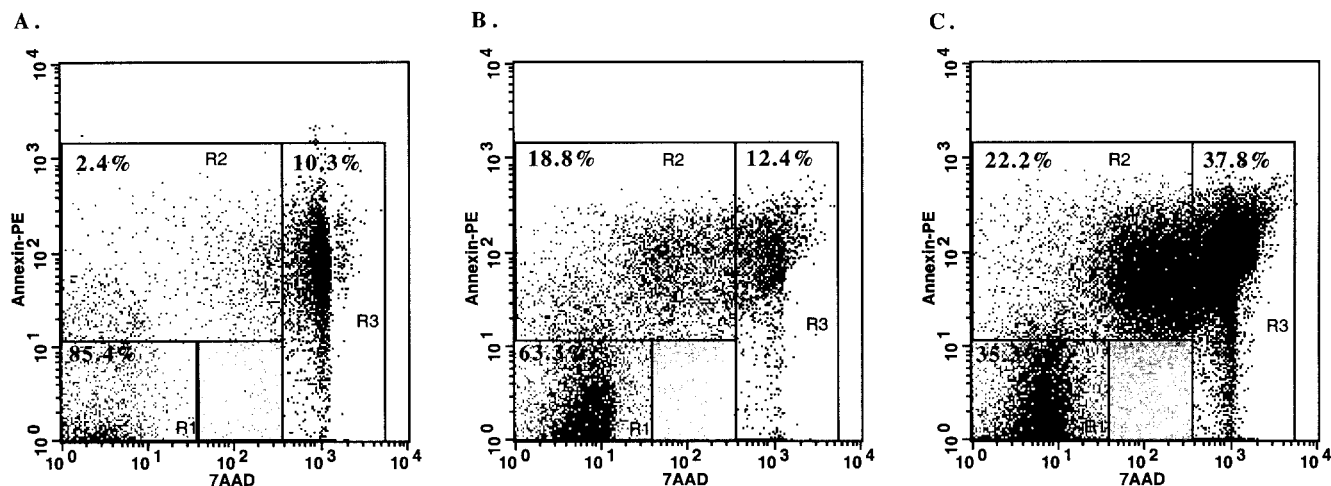


FIG. 6. Gating strategy for differentiation of live, apoptotic, and dead cells based upon Annexin V and 7AAD staining of *M. bovis* PPD-stimulated bovine PBMC. Mononuclear cells from *M. bovis*-infected (10^5 CFU) cattle were isolated and cultured with no stimulation (A), 5 μ g of PPD/ml (B), or 1 μ g of PWM/ml (C) for 5 days. Gates were set based on Annexin V and 7AAD staining properties in order to discriminate between live (R1, Annexin V⁻ 7AAD⁻), early apoptotic (R2, Annexin V⁺ 7AAD^{dim/-}), and dead (R3, Annexin V⁺ 7AAD^{bright}) cells. Values on plots represent percentages of cells within individual gates. Dot plots of Annexin V and 7AAD staining for a representative animal are provided, with similar staining patterns detected for other animals and for both staining protocols used for five-color analysis (i.e., with either the streptavidin-RED613 or streptavidin-ECD conjugate).

and chemokines produced by nearby mononuclear cells. The impact of chronic stimulation is not easily assessed *in vitro*. To address this limitation, we analyzed cells from persistently infected tissues as well as from tissues without evidence of mycobacterial colonization or lesions. Analysis of CD25, CD44, and CD62L expression by cells obtained from tuberculosis-affected organs of infected cattle compared to the same tissues from healthy cattle indicated that, as with the *in vitro* response, CD62L expression is down regulated by chronic activation and inflammation (Table 4). Likewise, calves infected with bovine respiratory syncytial virus exhibit decreased expression of CD62L on infiltrating bronchial lymph node T cells (36). In contrast to our present *in vitro* findings, CD44 expression on bovine T cells obtained from lungs of infected cattle was reduced (i.e., down regulated) compared to that of healthy controls (Table 4). Tonsillar and Peyer's patch (i.e., areas with chronic antigenic stimulation) CD4⁺ cells also exhibit reduced expression of bovine CD44 compared to that of CD4⁺ cells obtained from nonactivated parotid lymph nodes (44). Together, these findings suggest that in areas of chronic inflammation and activation, CD44 expression is down regulated on

bovine T cells. Alternatively, selective reductions of CD44^{high} cells by apoptosis or by other mechanisms may occur.

In a mouse model of rheumatoid arthritis, stimulation of CD44 by receptor-ligand binding of fragmented hyaluronan up regulates Fas expression, augmenting Fas-mediated apoptosis of CD44-expressing synovial cells (23). Additionally, concanavalin A (ConA)-activated T cells from CD44-deficient mice are more resistant to activation-induced apoptosis, and this "apoptosis resistance" enhances hepatitis upon ConA administration (14). Together, these findings support a recent hypothesis that apoptosis mediated via CD44 signaling is beneficial for regulation of inflammatory responses (14). As with rheumatoid arthritis, a balance between activation-induced apoptosis and activation-induced proliferation influences inflammation induced by the tubercle bacilli. Expression of and signaling through CD44 on inflammatory cells trafficking to infection sites likely modulate the severity of granulomatous inflammation. *M. bovis* BCG-infected mice initially have large expansions of CD44^{high} CD4⁺ T cells within infected tissues, followed by rapid reductions in the numbers of these activated T cells (17). Reductions in CD44^{high} CD4⁺ T-cell numbers

TABLE 3. Expression of CD44 (CY 5) on live and early apoptotic activated CD4⁺ cells^a

Animal no.	<i>M. bovis</i> PPD stimulated		PWM stimulated	
	Annexin V ⁻ 7AAD ⁻	Annexin V ⁺ 7AAD ^{dim/-}	Annexin V ⁻ 7AAD ⁻	Annexin V ⁺ 7AAD ^{dim/-}
408	356.1	172.4	286.4	7.6
410	322.7	124.5	294.4	7.3
426	188.8	143.9	207.8	5.5
Mean \pm SEM ^b	289.2 \pm 51.1*	146.9 \pm 13.9	262.9 \pm 27.6**	6.8 \pm 0.7

^a The geometric mean fluorescence (CY 5) intensity of CD44 was determined for CD4⁺ (i.e., PE⁺) and either Annexin V⁻ 7AAD⁻ (i.e., live) or Annexin V⁺ 7AAD^{dim/-} (i.e., early apoptotic) cells. Animals 408, 410, and 426 were aerosol infected (10^5 CFU) with *M. bovis*. Responses to PWM were from PBMC obtained from three noninfected animals.

^b *, differs ($P = 0.05$) from responses of PPD-stimulated, Annexin V⁺ 7AAD^{dim/-} cells; **, differs ($P = 0.002$) from responses of PWM-stimulated, Annexin V⁺ 7AAD^{dim/-} cells.

TABLE 4. Expression (PerCP) of CD44 and CD62L on mononuclear cells from tissues of *M. bovis*-infected and noninfected cattle^a

Expt group (n)	CD44 expression (MFI) in:		CD62L expression (MFI) in:	
	Lung	Mediastinal lymph node	Lung	Mediastinal lymph node
Infected (10)	11.2 ± 1.3***	24.0 ± 1.3	8.3 ± 0.9*	25.6 ± 1.4**
Noninfected (9)	24.4 ± 5.2	27.3 ± 4.5	14.1 ± 2.6	32.4 ± 1.4

^a Differences (*, $P < 0.05$; **, $P < 0.01$; ***, $P < 0.001$) from the mean fluorescence intensity (MFI) of the respective molecule (i.e., CD44 or CD62L) from the same tissue of noninfected cattle (i.e., vertical comparison) are indicated. Data are presented as means ± SEM. Differences ($P < 0.05$) in CD25 expression by cells collected from tissues of infected and noninfected cattle were not detected (data not shown).

result from IFN- γ -mediated apoptosis, as contractions in this population do not occur in IFN- γ knockout mice infected with *M. bovis* BCG. Mice lacking osteopontin, another ligand for CD44 and a proinflammatory cytokine, exhibit delayed clearance of *M. bovis* BCG and delayed resolution of associated inflammation compared to that of wild-type mice (39). Granulomata (i.e., size, number, and percent tissue affected) are increased in these mice, suggesting macrophage impairment and a role for lesion regression by osteopontin-CD44 interactions. While only speculative, CD44-mediated apoptosis also may regulate the numbers of activated T cells within tubercular lesions of cattle. Apoptosis of activated cells trafficking to areas of granulomatous inflammation would then serve to limit tissue damage caused by excessive production of inflammatory cytokines.

In summary, a robust recall proliferative response by bovine CD4⁺ cells to soluble mycobacterial antigens is corroborated by appropriate alterations in adhesion molecule and CD25 expression on these cells. Proliferation was linked with markedly increased expression of CD25 and CD44 and decreased expression of CD62L by bovine T cells. These alterations in cytokine receptor and adhesion molecule expression would impact trafficking and functional capacities of T cells proliferating in response to mycobacterial antigens. Additionally, activation-induced apoptosis of in vitro-stimulated CD4⁺ cells leads to significant decreases in CD44 expression, which may have important consequences in areas of chronic antigen stimulation. CD44 expression on T cells of tuberculosis-affected tissues was reduced in comparison to that of healthy animals. The functional relevance and correlation with in vitro findings, however, remain unclear.

ACKNOWLEDGMENTS

We thank Rebecca Lyon and Jody Mentele for technical support with pathology procedures and mycobacterial culture, respectively, and Nate Horman, Larry Wright, Dennis Weuve, Doug Ewing, and Wayne Varland for animal care.

REFERENCES

- Ahmed, R., and D. Gray. 1996. Immunological memory and protective immunity: understanding their relation. *Science* 272:54–60.
- Andersen, P., A. B. Andersen, A. L. Sorensen, and S. Nagai. 1995. Recall of long-lived immunity to *Mycobacterium tuberculosis* infection in mice. *J. Immunol.* 154:3359–3372.
- Andersen, P., and B. Smedegaard. 2000. CD4⁺ T-cell subsets that mediate immunological memory to *Mycobacterium tuberculosis* infection in mice. *Infect. Immun.* 68:621–629.

- Ashley, D. M., S. J. Bol, C. Waugh, and G. Kannourakis. 1993. A novel approach to the measurement of different *in vitro* leukaemic cell growth parameters: the use of PKH GL fluorescent probes. *Leuk. Res.* 17:873–882.
- Augustin, A., R. T. Kubo, and G. K. Sim. 1989. Resident pulmonary lymphocytes expressing the γ/δ T-cell receptor. *Nature* 340:239–241.
- Barrow, P. A., and J. Gallagher. 1981. Aspects of the epidemiology of bovine tuberculosis in badgers and cattle. I. The prevalence of infection in two wild animal populations in south-west England. *J. Hyg.* 86:237–245.
- Bolin, C. A., D. L. Whipple, K. V. Khanna, J. M. Risdahl, P. K. Peterson, and T. W. Molitor. 1997. Infection of swine with *Mycobacterium bovis* as a model of human tuberculosis. *J. Infect. Dis.* 176:1559–1566.
- Boom, W. H., K. A. Chervenak, M. A. Mincek, and J. J. Ellner. 1992. Role of the mononuclear phagocyte as an antigen-presenting cell for human γ/δ T cells activated by live *Mycobacterium tuberculosis*. *Infect. Immun.* 60:3480–3488.
- Burton, J. L., and M. E. Kehrli. 1996. Effects of dexamethasone on bovine circulating T lymphocyte populations. *J. Leukoc. Biol.* 59:90–99.
- Camp, R. L., A. Scheynius, C. Johansson, and E. Pure. 1993. CD44 is necessary for optimal contact allergic responses but is not required for normal leukocyte extravasation. *J. Exp. Med.* 178:497–507.
- Caruso, A. M., N. Serbina, E. Klein, K. Triebold, B. R. Bloom, and J. L. Flynn. 1999. Mice deficient in CD4 T cells have only transiently diminished levels of IFN- γ , yet succumb to tuberculosis. *J. Immunol.* 162:5407–5416.
- Chackerian, A. A., T. V. Perera, and S. M. Behar. 2001. Gamma interferon-producing CD4⁺ T lymphocytes in the lung correlate with resistance to infection with *Mycobacterium tuberculosis*. *Infect. Immun.* 69:2666–2674.
- Chao, C. C., M. Sandor, and M. O. Dailey. 1994. Expression and regulation of adhesion molecules by γ/δ T cells from lymphoid tissues and intestinal epithelium. *Eur. J. Immunol.* 24:3180–3187.
- Chen, D., R. J. McKallip, A. Zeytun, Y. Do, C. Lombard, J. L. Robertson, T. W. Mak, P. S. Nagarkatti, and M. Nagarkatti. 2001. CD44-deficient mice exhibit enhanced hepatitis after concanavalin A injection: evidence for involvement of CD44 in activation-induced cell death. *J. Immunol.* 166:5889–5897.
- Coleman, J. D. 1988. Distribution, prevalence and epidemiology of bovine tuberculosis in brushtail possums, *Trichosurus vulpecula*. *Austr. Wildl. Res.* 15:651–663.
- Dailey, M. O. 1998. Expression of T lymphocyte adhesion molecules: regulation during antigen-induced T cell activation and differentiation. *Immunology* 18:153–184.
- Dalton, D. K., L. Haynes, C. Q. Chu, S. L. Swain, and S. Wittmer. 2000. Interferon- γ eliminates responding CD4 T cells during mycobacterial infection by inducing apoptosis of activated CD4 T cells. *J. Exp. Med.* 192:117–122.
- Doherty, M. L., H. F. Bassett, P. J. Quinn, W. C. Davis, A. P. Kelly, and M. L. Monaghan. 1996. A sequential study of the bovine tuberculin reaction. *Immunology* 87:9–14.
- D'Souza, C. D., A. M. Cooper, A. A. Frank, R. J. Mazzaccaro, B. R. Bloom, and I. M. Orme. 1997. An anti-inflammatory role for gamma delta T lymphocytes in acquired immunity to *Mycobacterium tuberculosis*. *J. Immunol.* 158:1217–1221.
- Feng, C. G., A. G. Bean, H. Hooi, H. Briscoe, and W. J. Britton. 1999. Increase in gamma interferon-secreting CD8⁺, as well as CD4⁺, T cells in lungs following aerosol infection with *Mycobacterium tuberculosis*. *Infect. Immun.* 67:3242–3247.
- Flynn, J. L., and J. Chan. 2001. Immunology of tuberculosis. *Annu. Rev. Immunol.* 19:93–129.
- Flynn, J. L., M. M. Goldstein, K. J. Triebold, B. Koller, and B. R. Bloom. 1992. Major histocompatibility complex class I-restricted T cells are required for resistance to *Mycobacterium tuberculosis* infection. *Proc. Natl. Acad. Sci. USA* 89:12013–12017.
- Fujii, K., Y. Fujii, S. Hubscher, and Y. Tanaka. 2001. CD44 is the physiological trigger of Fas up-regulation on rheumatoid synovial cells. *J. Immunol.* 167:1198–1203.
- Griffin, J. P., and I. M. Orme. 1994. Evolution of CD4 T-cell subsets following infection of naive and memory immune mice with *Mycobacterium tuberculosis*. *Infect. Immun.* 62:1683–1690.
- Griffin, J. P., K. V. Harshan, W. K. Born, and I. M. Orme. 1991. Kinetics of accumulation of gamma delta receptor-bearing T lymphocytes in mice infected with live mycobacteria. *Infect. Immun.* 59:4263–4265.
- Hamann, A., D. Jablonski-Westrich, K. U. Scholz, A. Duijvestijn, E. C. Butcher, and H. Thiele. 1988. Regulation of lymphocyte homing. I. Alterations in homing receptor expression and organ-specific high endothelial venule binding of lymphocytes upon activation. *J. Immunol.* 140:737–743.
- Howard, A. D., O. J. Trask, S. E. Weisbrode, and B. S. Zwilling. 1998. Phenotypic changes in T cell populations during the reactivation of tuberculosis in mice. *Clin. Exp. Immunol.* 111:309–315.
- Howard, C. J., P. Sopp, and K. R. Parsons. 1992. L-selectin expression differentiates T cells isolated from different lymphoid tissues in cattle but does not correlate with memory. *Immunology* 77:228–234.
- Janis, E. M., S. H. E. Kaufmann, R. H. Schwartz, and D. M. Pardoll. 1989.

- Activation of $\gamma\delta$ T cells in the primary immune response to *Mycobacterium tuberculosis*. *Science* **244**:713–716.
30. Jung, T. M., W. M. Gallatin, I. L. Weissman, and M. O. Dailey. 1988. Down-regulation of homing receptors after T cell activation. *J. Immunol.* **141**:4110–4117.
 31. Lalvani, A., R. Brookes, R. J. Wilkinson, A. S. Malin, A. A. Pathan, P. Andersen, H. Dockrell, G. Pasvol, and A. V. S. Hill. 1998. Human cytolytic and interferon γ -secreting CD8⁺ T lymphocytes specific for *Mycobacterium tuberculosis*. *Proc. Natl. Acad. Sci. USA* **95**:270–275.
 32. Liebana, E., R. M. Girvin, M. Welsh, S. D. Neill, and J. M. Pollock. 1999. Generation of CD8⁺ T-cell responses to *Mycobacterium bovis* and mycobacterial antigen in experimental bovine tuberculosis. *Infect. Immun.* **67**:1034–1044.
 33. Lukey, P. T., S. E. Latouf, and S. R. Ress. 1996. Memory lymphocytes from tuberculous effusions: purified protein derivative (PPD) stimulates accelerated activation marker expression and cell cycle progression. *Clin. Exp. Immunol.* **104**:412–418.
 34. Lyadova, I. V., E. B. Eruslanov, S. V. Khaidukov, V. V. Yeremeev, K. B. Majorov, A. V. Pichugin, B. V. Nikonenko, T. K. Kondratieva, and A. S. Apt. 2000. Comparative analysis of T lymphocytes recovered from the lungs of mice genetically susceptible, resistant, and hyperresistant to *Mycobacterium tuberculosis*-triggered disease. *J. Immunol.* **165**:5921–5931.
 35. Lyadova, I., V. Yeremeev, K. Majorov, B. Nikonenko, S. Khaidukov, T. Kondratieva, N. Kobets, and A. Apt. 1998. An ex vivo study of T lymphocytes recovered from the lungs of I/St mice infected with and susceptible to *Mycobacterium tuberculosis*. *Infect. Immun.* **66**:4981–4988.
 36. McInnes, E., P. Sopp, C. J. Howard, and G. Taylor. 1999. Phenotypic analysis of local cellular responses in calves infected with bovine respiratory syncytial virus. *Immunology* **96**:396–403.
 37. Modlin, R. L., C. Pirmez, F. M. Hofman, V. Torigian, K. Uyemura, T. H. Rea, B. R. Bloom, and M. B. Brenner. 1989. Lymphocytes bearing antigen-specific gamma delta T-cell receptors accumulate in human infectious disease lesions. *Nature* **339**:544–548.
 38. Muller, I., S. P. Cobbold, H. Waldmann, and S. H. E. Kaufmann. 1987. Impaired resistance to *Mycobacterium tuberculosis* infection after selective in vivo depletion of L3T4⁺ and Lyt2⁺ T cells. *Infect. Immun.* **55**:2037–2041.
 39. Nau, G. J., L. Liaw, G. L. Chupp, J. S. Berman, B. L. Hogan, and R. A. Young. 1999. Attenuated host resistance against *Mycobacterium bovis* BCG infection in mice lacking osteopontin. *Infect. Immun.* **67**:4223–4230.
 40. Ng, K. H., F. E. Aldwell, D. N. Wedlock, J. D. Watson, and B. M. Buddle. 1997. Antigen-induced interferon-gamma and interleukin-2 responses of cattle inoculated with *Mycobacterium bovis*. *Vet. Immunol. Immunopathol.* **57**: 59–68.
 41. Orme, I. M., and F. M. Collins. 1983. Protection against *Mycobacterium tuberculosis* infection by adoptive immunotherapy: requirement for T cell-deficient recipients. *J. Exp. Med.* **158**:74–83.
 42. Pedrazzini, T., K. Hug, and J. A. Louis. 1987. Importance of L3T4⁺ and Lyt-2⁺ cells in the immunologic control of infection with *Mycobacterium bovis* strain bacillus Calmette-Guerin in mice: assessment by elimination of T cell subsets *in vivo*. *J. Immunol.* **139**:2032–2037.
 43. Quade, M. J., and J. A. Roth. 1999. Dual-color flow cytometric analysis of phenotype, activation marker expression, and proliferation of mitogen-stimulated bovine lymphocyte subsets. *Vet. Immunol. Immunopathol.* **67**:33–45.
 44. Rebelatto, M. C., C. Mead, and H. HogenEsch. 2000. Lymphocyte populations and adhesion molecule expression in bovine tonsils. *Vet. Immunol. Immunopathol.* **73**:15–29.
 45. Rhodes, S. G., D. Gavier-Widen, B. M. Buddle, A. O. Whelan, M. Singh, R. G. Hewinson, and H. M. Vordermeier. 2000. Antigen specificity in experimental bovine tuberculosis. *Infect. Immun.* **68**:2573–2578.
 46. Sacco, R. E., R. J. Jensen, C. O. Thoen, M. Sandor, J. Weinstock, R. G. Lynch, and M. O. Dailey. 1996. Cytokine secretion and adhesion molecule expression by granuloma T lymphocytes in *Mycobacterium avium* infection. *Am. J. Pathol.* **148**:1935–1948.
 47. Schmitt, S. M., S. D. Fitzgerald, T. M. Cooley, C. S. Bruning-Fann, L. Sullivan, D. Berry, T. Carlson, R. B. Minnis, J. B. Payeur, and J. Sikarskie. 1997. Bovine tuberculosis in free-ranging white-tailed deer from Michigan. *J. Wildl. Dis.* **33**:749–758.
 48. Serbina, N. V., and J. L. Flynn. 2001. CD8⁺ T cells participate in the memory immune response to *Mycobacterium tuberculosis*. *Infect. Immun.* **69**:4320–4328.
 49. Serbina, N. V., V. Lazarevic, and J. L. Flynn. 2001. CD4⁺ T cells are required for the development of cytotoxic CD8⁺ T cells during *Mycobacterium tuberculosis* infection. *J. Immunol.* **167**:6991–7000.
 50. Shigenaga, T., A. M. Dannenberg, D. B. Lowrie, W. Said, M. J. Urist, H. Abbey, B. H. Schofield, P. Mounts, and K. Sugisaki. 2001. Immune responses in tuberculosis: antibodies and CD4-CD8 lymphocytes with vascular adhesion molecules and cytokines (chemokines) cause a rapid antigen-specific cell infiltration at sites of bacillus Calmette-Guerin reinfection. *Immunology* **102**:466–479.
 51. Smith, R. A., J. M. Kreeger, A. J. Alvarez, J. C. Goin, W. C. Davis, D. L. Whipple, and D. M. Estes. 1999. Role of CD8⁺ and WC-1⁺ $\gamma\delta$ T cells in resistance to *Mycobacterium bovis* infection in the SCID-bo mouse. *J. Leukoc. Biol.* **65**:28–34.
 52. Smyth, A. J., M. D. Welsh, R. M. Girvin, and J. M. Pollock. 2001. In vitro responsiveness of $\gamma\delta$ T cells from *Mycobacterium bovis*-infected cattle to mycobacterial antigens: predominant involvement of WC1⁺ cells. *Infect. Immun.* **69**:89–96.
 53. Storset, A. K., G. Berntsen, and H. J. Larsen. 2000. Kinetics of IL-2 receptor expression on lymphocyte subsets from goats infected with *Mycobacterium avium* subsp. *paratuberculosis* after specific *in vitro* stimulation. *Vet. Immunol. Immunopathol.* **77**:43–54.
 54. Tanaka, Y., C. T. Morita, Y. Tanaka, E. Nieves, M. B. Brenner, and B. R. Bloom. 1995. Natural and synthetic non-peptide antigens recognized by human $\gamma\delta$ T cells. *Nature* **375**:155–158.
 55. Walcheck, B., and M. A. Jutila. 1994. Bovine $\gamma\delta$ T cells express high levels of functional peripheral lymph node homing receptor (L-selectin). *Int. Immunol.* **6**:81–91.
 56. Waters, W. R., J. R. Stabel, R. E. Sacco, J. A. Harp, B. A. Pesch, and M. J. Wannemuehler. 1999. Antigen-specific B-cell unresponsiveness induced by chronic *Mycobacterium avium* subsp. *paratuberculosis* infection of cattle. *Infect. Immun.* **67**:1593–1598.
 57. Waters, W. R., M. V. Palmer, B. A. Pesch, S. C. Olsen, M. J. Wannemuehler, and D. L. Whipple. 2000. Lymphocyte subset proliferative responses of *Mycobacterium bovis*-infected cattle to purified protein derivative. *Vet. Immunol. Immunopathol.* **77**:257–273.
 58. Waters, W. R., B. J. Nonnecke, T. E. Rahner, M. V. Palmer, D. L. Whipple, and R. L. Horst. 2001. Modulation of *Mycobacterium bovis*-specific responses of bovine peripheral blood mononuclear cells by 1,25-dihydroxyvitamin D₃. *Clin. Diagn. Lab. Immunol.* **8**:1204–1212.